J. Membrane Biol. 198, 77–87 (2004)
DOI: 10.1007/s00232-004-0661-3

The Journal of
Membrane
Biology

Gadolinium Effects on Gigaseal Formation and the Adhesive Properties of a Fungal Amoeboid Cell, the *Slime* Mutant of *Neurospora crassa*

A.Y. Dunina-Barkovskaya[1], **N.N. Levina**[2], **R.R. Lew**[2], **I.B. Heath**[2]
[1]A.N. Belozersky Institute, Moscow State University, 119899, Moscow, Russia
[2]Department of Biology, York University, 4700 Keele Street, Toronto, Ontario, M3 J 1P3, Canada

Received: 21 August 2003/Revised: 23 January 2004

Abstract. Low gadolinium concentrations induce rapid gigaseal formation and cell adhesion to glass and plastic (polystyrene) substrates in the *slime* mutant of *Neurospora crassa*. Cellular adhesion is independent of an integrin-mediated mechanism, because pretreatment with the oligopeptide ARG-GLY-ASP-SER (RGDS) did not inhibit it, and there was no spatial correlation between integrin and adhesions. In contrast, concanavalin A and *beta*-galactosidase both inhibit adhesion, suggesting that adhesion is mediated by sugar moeities at the cell surface. The adhesion sites are motile in the plasma membrane, as shown by the movement of polystyrene microspheres on the cell surface. In addition to an integrin-based adhesive system, which has already been characterized in walled hyphal cells, hyphae have evolved at least two different plasma membrane-based adhesion mechanisms. The relatively non-specific sugar-mediated adhesion caused by gadolinium may be part of the mechanism of gigaseal formation in other cells. In the absence of sugar-mediated adhesion, gadolinium increases the magnitude of the gigaseal in giant unilamellar liposomes composed of phosphatidylcholine, phosphatidylethanolamine, and cholesterol, with or without the negatively charged phosphatidylserine. Thus, gigaseal formation involves at least two different mechanisms.

Correspondence to: R.R. Lew; email: planters@yorku.ca

Abbreviations: BTP, bis-tris-propane; MES, morpholinoethanesulfonic acid; RGDS and RGDE, oligopeptides ARG-GLY-ASP-SER and ARG-GLY-GLU-SER, respectively; BS, bath solution; BSA, bovine serum albumin; PBS, phosphate-buffered saline; GULs, giant unilamellar liposomes; PC, Palmitoyl-2-linoleoyl-sn-glycero-3-phosphocholine; PE, 1-Palmitoyl-2-linoleoyl-sn-glycero-3-phosphoethanolamine; PS, 1-Palmitoyl-2-linoleoyl-sn-glycero-3-[phospho-L-serine] (sodium salt); Ch, Cholesterol.

Key words: *Slime* mutant — Amoeboid cells — *Neurospora crassa* — Gigaseal formation — Adhesion — Gadolinium

Introduction

During patch-clamp studies of blue light modulation of ion transport we discovered that low [Gd^{3+}] induces rapid formation of gigaseals in *slime* cells (Levina et al., 2002). Little is known about the formation of the high-resistance contact between the cell membrane and glass pipette (gigaseal), even though gigaseals are used commonly in patch-clamp experiments. Sachs and Qin (1993) have observed channel-like behavior in high-resistance glass-hydrophobic surface interfaces, suggesting the presence of structures capable of passing ions, structures that can have properties similar to ion channels. Most research on gigaseals has focussed on the structure of the membrane patch. There are significant morphological changes of the plasma membrane leading to formation of the seal (Sokabe & Sachs, 1990; Ruknudin, Song & Sachs, 1991). The area of contact between the glass and membrane may be varied without affecting the gigaseal resistance, implying that the resistance per unit length of membrane/glass contact is very high. Sokabe and Sachs (1990) proposed a model of denatured protein and high density of glycoprotein sugar residues contacting the glass and creating a high-resistance zone analogous to a sucrose gap that blocks movement of ions. The appearance of lipid blebs in the pipette upon applying suction led to the suggestion that the seal is formed between the lipid surface and the glass (Milton & Caldwell, 1990), a reasonable possibility since patch-clamped liposomes form gigaseals readily (Tank, Miller & Webb, 1982). However, the possible relationship between gigaseal formation and cell adhesion to substrates has not previously been explored to our knowledge.

The interaction between a cell and its surroundings is mediated, at least to some degree, by plasma membrane-based mechanisms. Such mechanisms include adhesion to diverse substrates and are important to the biology of animal cells in processes such as amoeboid movement. The significance of plasma membrane adhesion to plant and fungal cells normally encased in a cell wall is less evident, although there is growing evidence of a functional role in these cells, too (Heath, 2001). Normally, plasma membrane adhesion of walled cells is difficult to study in relatively unmanipulated cells because of the close apposition of plasma membrane and cell wall generated by turgor pressure. The *slime* mutant of *Neurospora crassa*, first described by Emerson (1963), presents a novel opportunity to study adhesion because it has a cell wall-less amoeboid cell phenotype. Such a phenotype is unusual, perhaps unique within the fungal kingdom, which is characterized by walled cells under high hydrostatic pressure. The presence of amoeboid capability within the fungal kingdom has been used in support of the proposition that hyphal cells grow like an amoeba in a tube (Reinhardt, 1892; Heath & Steinberg, 1999). The cell wall-less phenotype makes it possible to perform patch-clamp experiments with relative ease (Levina et al., 2002). *Slime* has also been used extensively to characterize purified plasma membranes (*cf* Scarborough, 1975; Bowman & Slayman, 1977).

We took advantage of the Gd^{3+} effect on *slime* cells and characterized both gigaseal formation and adhesions monitored by interference-reflection microscopy. In doing so, we observed an adhesive mechanism, separate and distinct from integrin-mediated adhesion, which appears to involve sugar residues on the cell surface and may aid the formation of the gigaseal. Gd^{3+} also increases the resistance of pre-existing gigaseals on giant unilamellar liposomes.

Materials and Methods

Cell Culture

The *slime* mutant of *Neurospora crassa* was obtained from G. Scarborough (University of North Carolina). Genetically, *slime* consists of three mutations (*fz, sg, os-1*). Two, *fz* and *sg*, have not been cloned and their identity is unknown. The *fz* (fuzzy) mutant exhibits abnormal morphology; the *sg* (spontaneous germination) mutant exhibits poor growth and ascospores that germinate without heat shock (Perkins et al., 1982). The third mutation of *slime*,*os-1*, is now known to be the same as *nik-1* (Schumacher, Enderlin & Selitrennikoff, 1997). *Nik-1* shares homology with the kinase and regulator modules of two component histidine kinases (Alex, Borkovich & Simon, 1996); the *nik-1* mutant exhibits aberrant colonial-type growth, especially at high extracellular osmolarity, suggesting a role in osmo-sensing and response (Alex et al., 1996; Schumacher et al., 1997).

Stocks were stored and cultures maintained as described in Levina et al. (2002). Briefly, stock cultures were maintained by storage on agar slants (Bowman & Slayman, 1977). An aliquot from the stock cultures was used to inoculate a liquid culture that was grown with gentle shaking (50 rpm) at 30°C for 24 hours. Aliquots of the liquid culture were then used to inoculate fresh agar slants (1% w/v agar). For both agar slants and liquid cultures, the growth medium (GM) consisted of Vogel's N medium (Vogel, 1956) supplemented with 2% (w/v) mannitol, 0.75% (w/v) yeast extract, and 0.75% (w/v) nutrient broth (Difco, Detroit, MI).

Cell Preparation

For experiments, cells from a slant culture were inoculated into 30 ml of GM and incubated in the shaker (50 rpm) at 30°C overnight. In the morning, 0.5–1 ml of the culture was transferred into 30 ml of fresh GM and incubated for 1–5 hours (30°C). The cells were centrifuged at $2,600 \times g$ for about 5 seconds, washed twice with bath solution (BS), and resuspended in 1 ml of BS. This cell suspension was used as a stock for patch-clamp and adhesion experiments. BS contained, in mM: 50 KCl, 1 $CaCl_2$, 10 MES/BTP, pH 5.8, and either 1 $MgCl_2$ (BS-1) or 50 $MgCl_2$ (BS-50); osmolality was adjusted with sorbitol to 350 mosmol/kg.

Gigaseal Measurements

For patch-clamp experiments, cells (20 μl) were transferred into the experimental chamber containing 2 ml of BS-50. Cells used for patching were of variable size, with diameter between 8 and 25 μm. We chose non-vacuolated, initially spherical cells, which became amoeba-like after they attached to the bottom, but had not yet formed pseudopodia. Seals were usually achieved within 30–40 min after the patch pipette was pressed against the cell surface and the initially applied positive pressure was released.

The electrophysiology setup was described in detail in Levina et al. (2002). Patch pipettes were fabricated from borosilicate tubing (Warner Instruments, Hamden, CT) on a vertical puller (P-30, Sutter Instruments, USA). Salt bridges (1% agar) used KCl concentrations matched to the pipette [Cl^-] to minimize junction potentials. Gigaseal formation was monitored using a Dagan patch-clamp amplifier (Model 8900, Dagan, Minneapolis, MN) before and after addition of 0.5 mM $GdCl_3$, added directly to the experimental chamber by gradual addition of stock solution.

Cell Adhesion to Substrate

Aliquots of liquid-grown slime were re-inoculated into fresh liquid medium, and grown for 1–5 h at 30°C to reach a cell density of 1×10^6 cells/ml. The cell suspension (1 ml) was centrifuged at $2,600 \times g$ for 5 s, re-suspended in 1 ml of BS-1 or BS-50, and incubated for 15–30 min at 30°C with gentle shaking. For adhesion experiments, a 50 μl aliquot of cells was added into 2 ml of BS-1 or BS-50 in the chamber, which had a pre-cleaned glass cover slip on the bottom.

After placing cells into the chamber they were observed under a 40× water immersion objective on an Olympus confocal microscope. Usually, three different fields of view were recorded at specific time points. The percentage of adhered cells was calculated as the ratio of adhered cells (*see* below) to the total number of cells in the field of view. We examined 3–4 fields of view for each time point. Usually, 2–3 separate preparations were analyzed. A number of substrates were used in addition to pre-cleaned glass cover slips: gelatin, BSA, poly-L-lysine, pronectin F and polystyrene. Gelatin-coated glass was prepared by covering glass cover slips with 0.02% gelatin in PBS, left overnight at room temperature, washed with dH_2O, then dried. The same procedure was used for cover slips coated with 3% BSA (no attachment was observed) and 1% poly-L-lysine (attachment was observed, but not measured). Pronectin

F-coated 35 × 10 mm tissue culture dishes were obtained from ICN Biomedicals (Costa Mesa, CA) (SMARTPLASTIC™, catalog number 7690103). ProNectin F is a recombinant polypeptide with a crystalline, silk-like backbone containing multiple ARG-GLY-ASP (RGD) repeats—cell attachment sites from human fibronectin. The plastic substrate was polystyrene tissue culture dishes (Falcon, 35 × 10 mm, catalog number 3001).

In experiments with RGDS (ARG-GLY-ASP-SER) and RGES (ARG-GLY-GLU-SER), the peptides were added into the cell suspension in BS-50 to a final concentration of 5 mM and cells were incubated with shaking at 30°C for 30–40 min. Then, 50 μl of the cell suspension was added to 2 ml BS-50 and adhesion monitored. RGDS (catalog number A-9041) and RGES (catalog number A-5686) were both from Sigma.

Concanavalin A from *Canavalia ensiformis* (ConA, L-7647, Sigma, St. Louis, MO) was added to final concentration of 40 μg/ml into the cell suspension, and the cells were incubated for 5–15 min at 30°C with gentle shaking. Longer incubation times caused cell aggregation and misshapen cells. We also used a ConA tetramethylrhodamine conjugate (excitation 555 nm, emission 580 nm) (C-860, Molecular Probes, Eugene, OR) to visualize localization of ConA binding sites, and compare ConA-treated and untreated cell adhesion. *Beta*-Galactosidase (G-5160, Sigma) was added to BS-50 to a final concentration of 200 units/ml and cells incubated at 30°C for 10 min. $GdCl_3$ was gently added by 2 μl drops from a 10 mM stock solution up to final concentration 100–500 μM into 2 ml of BS-1 or BS-50 in the chamber.

To observe microsphere adhesion, we used fluorescent carboxylate-modified polystyrene microspheres (1 μm diameter, excitation 580 nm, emission 605 nm) (F-8821, Molecular Probes). An aliquot of cells was added into the chamber, and the microspheres were added after the cells had settled to the bottom (about 30–40 min later). The beads were added to a final concentration of $\sim 10^6$ beads/ml from a stock of 3.6×10^{10} beads/ml. The cell density was $\sim 2.5 \times 10^4$ cells/ml (10–100 beads/cell).

Microscopy

We used a confocal scanning-type laser-reflected fluorescence microscope (Olympus, USA), equipped with red laser (633 nm) (reflectance mode, to observe adhesion and microspheres) and green laser (543 nm) (to observe tetramethylrhodamine ConA), in combined reflectance and fluorescence confocal microscopy. Imaging was performed with a 40× water immersion objective and various digital magnifications using Fluoview software (Olympus). To study adhesion of cells, we used the interference reflection technique (*cf* Izzard & Lochner, 1976; Opas, 1978). With this technique, zones of adhesion are visible as a dark area at the interface of the glass cover slip and the underside of the cell (http://www.olympusmicro.com/primer/techniques/fluorescence/tirf/tirf-references.html). Cells were scored as adhering if 50% of the cell 'bottom' exhibited dark coloration.

Immunocytochemistry

Cells were allowed to adhere to the cover slips for 15–20 min. Then, cells were prepared via a 'slow' freezing method (modified from Bourett, Czymmek & Howard, 1998). Cover slips with adhering cells were plunged upside down into acetone at −80°C to facilitate the permeabilization of the cells. After a few seconds of freezing in acetone, the cover slips were rinsed 3 times in ethanol (5 min each rinse) (at −80°C) and then transferred into 2% paraformaldehyde in ethanol (at −80°C). Solutions were changed by transferring stainless steel mesh baskets with vertically positioned cover slips from one flask to another. Samples were kept in this solution for 2 h before allowing the samples to warm up to room temperature. The samples then were rehydrated through a series of ethanol dilutions in PBS (phosphate-buffered saline, pH 7.1–7.2) and used for labelling with antibodies. Rehydrated samples were washed for 5 min in 0.01% Triton X-100 in PBS, treated with a blocking solution containing 10% normal goat serum and 3% bovine serum albumin in PBS for 60 min, and incubated in primary antibody for 2 h at room temperature. Antibodies were diluted in the PBS blocking solution as follows: 1:200 for anti-*beta*1-integrin subunit antibodies (CSAT, ascites; antibodies against chicken *beta*1-integrin subunit, developed in mouse; obtained from Developmental Studies Hybridoma Bank, The University of Iowa, IA). After incubation with primary antibodies, samples were rinsed for 5 min in PBS, 5 min in 0.01% Triton X-100 in PBS, then for 10 min with blocking solution. For immunolocalization, samples were incubated for 2 h in the dark at room temperature in the goat anti-mouse FITC-conjugated secondary antibodies diluted 1:100 (anti-mouse IgG, BioShop, Canada), rinsed 3× for 5 min with PBS and mounted with ProLong antifade agent (P-7481, Molecular Probes), and viewed on the FluoView confocal microscope.

Electron Scanning Microscopy

Cells were allowed to adhere to the cover slips for 15–20 min. Then, cells were prepared as described above. The specimens were coated with 60:40 Au:Pd, and scanned on a Hitachi 5520 scanning electron microscope at 20 kV with a 45° tilt.

Liposome Preparation and Patching

Giant unilamellar liposomes (GULs) were formed from a mixture of four phospholipids: PC, PE, PS and Cholesterol (Ch). Phospholipids in chloroform were mixed in a small glass vessel at a ratio PC:PE:PS:Ch = 50:10:30:10 (w/w). 20 μl aliquots were placed on pre-cleaned glass coverslips. Coverslips were placed into a vacuum desiccator for at least 12 h to let chloroform completely evaporate. After that, a 20-μl droplet of dH_2O was applied onto the dried phospholipids and left for at least 45 min to re-hydrate. GULs appeared as giant blackish blebs of 10–100 μm in diameter at the edges of the phospholipid droplet. Then coverslips were placed on the bottom of the recording chamber, 2 ml of BS added and GULs were patched within 15–30 min. Gigaseal formation was monitored in voltage-clamp mode by applying 250-ms 20-mV voltage pulses at a frequency of 1 Hz. Pipette solution was the same as for experiments of patching slime cells, except that nystatin was absent.

Giant unilamellar liposomes consisting of the same phospholipids but lacking PS (GUL(-S)) were prepared using the same protocol; the phospholipid ratio in the GUL(-S) was PC:PE:Ch = 20:70:10 (w/w). All lipids were purchased from Avanti Polar Lipids (USA).

Results

Gadolinium-induced Gigaseal Formation in *slime* Cells

Normally, gigaseal formation after appressing the patch pipette to the slime cell membrane is very slow, often requiring an hour or so (Levina et al., 2002). With the addition of 0.5–1.0 mM $GdCl_3$, a gigaseal was achieved very rapidly, within 5 minutes (Fig. 1).

Table 1. Cell adhesion to substrate after treatment

Substrate and Treatment	$-GdCl_3$ (control attachment)	$+GdCl_3$ (100–500 μM)
Glass	80% attachment after ~30 min (~20% attachment after 30 min in 1 mM $MgCl_2$)	100% attachment after 20–90 sec (~100% attachment after 20–90 s in 1 mM $MgCl_2$)
Glass + 5 mM RGDS (30 min pre-incubation	~80% attachment after ~30 min (115/142 [control[1]:76/102])	n.d.[2]
Glass + 5 mM RGES (30 min pre-incubation	~80% attachment after ~20 min (67/147 [control:65/84])	n.d.
Pronectin-coated glass	No attachment (0/147 [control: 72/95])	~100% attachment within ~90 sec (92/95)
Glass + 250 μM $GdCl_3$ (30 min pre-incubation)	No attachment; cells aggregated and mis-shapen	n.d.
Glass + 100 units/ml beta-galactosidase	No attachment (0/43)	No attachment (0/33)
Glass + 40 μg/ml Rh-ConA (30 min pre-incubation)	No attachment	Partial area attachment in 2.5 mM $GdCl_3$ (10/13)
Glass + 200 μg/ml ConA (30 min pre-incubation)	No attachment (30 min: 0/39; 50 min: 0/51)	No attachment (10 min: 0/97; 20 min: 0/57)
Plastic (polystyrene)	No attachment (1/89)	100% attachment after ~60 sec (43/43)
Plastic (polystyrene) + 200 μg/ml ConA (30 min pre-incubation)	No attachment (~30 min) (0/39)	No attachment (0/97)
Gelatin on glass	No attachment (0/161)	No attachment (0/214)

Adhesion was scored by counting the number of cells adhering to the substrate on the basis of interference reflection microscopy (*see* Fig. 2) as a percentage of the total number of cells. Multiple fields of view were examined. Examples of quantitations are shown as adhering cells/total cells and are representative examples of replicated experiments.
[1]Control adhesion of the same cell suspension to glass.
[2]n.d. not determined.

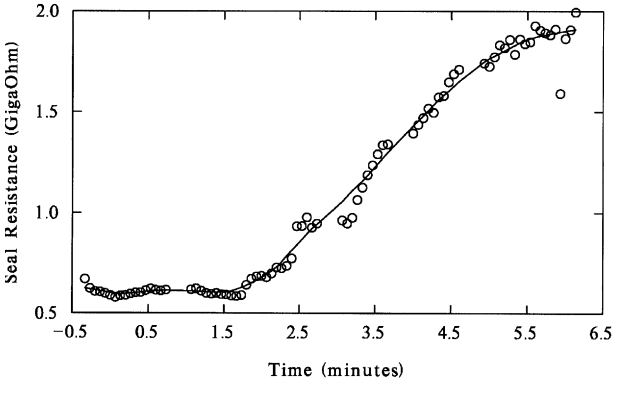

Fig. 1. Gigaseal formation. Seal formation was monitored by clamping the voltage to −100, 0 and 100 mV. The seal resistance was calculated by linear regression of the clamping currents at the three voltages. $GdCl_3$ (final concentration ~500 μM) was added to the tissue culture dish at time 0. Within 2 minutes it had diffused to the patch, causing increased seal resistance, which stabilized at about 2 GΩ.

Cellular Adhesion: High $[Mg^{2+}]$-Induced Attachment

We examined adhesion in the presence of high $[Mg^{2+}]$ because it enhances gigaseal formation on *slime* cells (Levina et al., 2002). Cellular adhesion was measured by monitoring the appearance of a close connection between the cell membrane and the substrate, using interference-reflection microscopy. For multiple fields of view, adhesion was scored as the number of adhering cells/total cells.

Slime cells readily attached to glass substrates. The rate of attachment and efficiency of attachment depended upon the concentration of $MgCl_2$ (Figs. 2, 3; Table 1). In the presence of 50 mM $MgCl_2$ (control conditions) (Fig. 2), about 50% of the cells attached to the surface within 16 minutes. Attachment increased to 80% after about 30 minutes (Fig. 3), and did not change within 1 hour. With longer incubation (overnight), attachment was complete, and the cells exhibited a flattened 'pancake' shape (Fig. 4). The time course of attachment was similar with lower concentrations of $MgCl_2$ (1 mM), but the maximum attachment efficiency was lower, about 20% (Fig. 3).

To assess the role of integrin in the attachment process (Hynes, 1992), the cells were pre-treated for 30–40 min with RGDS or RGES (5 mM). Neither pre-treatment affected attachment efficiency (Table 1). This suggests that integrin is not involved in the adhesive mechanism. We confirmed this by examining adhesion to gelatin-coated and pronectin-coated dishes. Pronectin is a recombinant protein containing RGD repeats. Adhesion to both gelatin and pronectin is supposed to involve RGD receptors (integrins). No attachment of *slime* cells on these

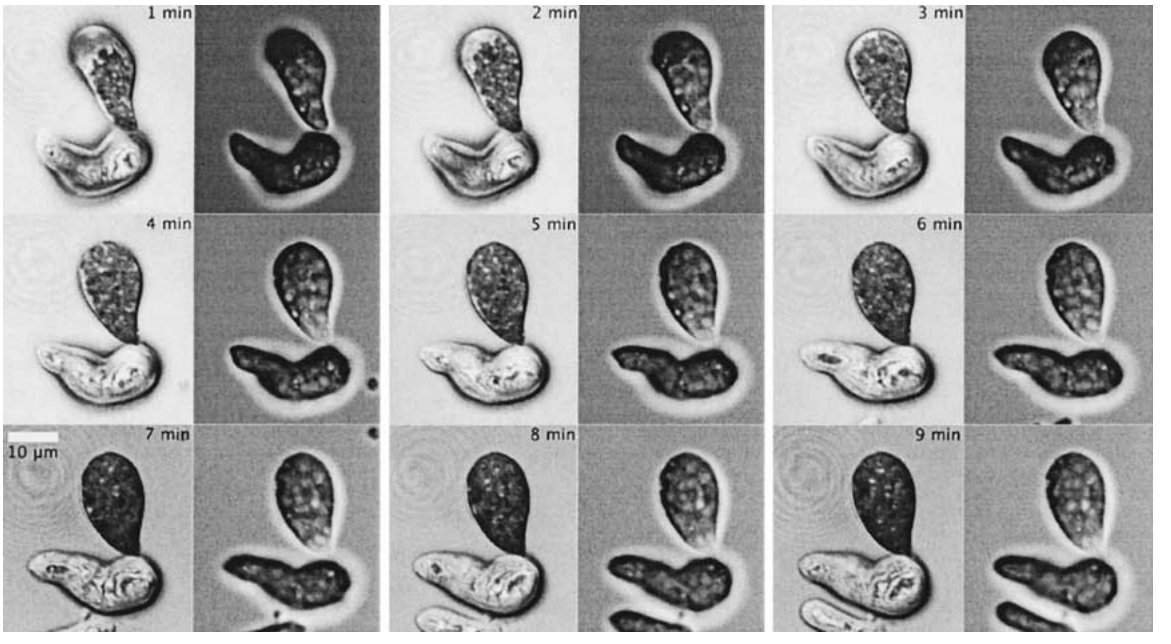

Fig. 2. Time dependence of *slime* cell adhesion in the presence of 50 mM $MgCl_2$. Interference reflection and DIC microscopy. Both the interference reflection (left panel of each figure pair) and DIC (right panel of each figure pair) images are shown for the times indicated. Adhesion causes dark coloration in the interference reflection microscopic images. Note that the upper cell achieves complete adhesion after 7 minutes, while the lower cell exhibits transient adhesion points, but does not adhere completely. For the quantitation in Table 1, cells were scored as adhering if 50% of the cell 'bottom' exhibited dark coloration.

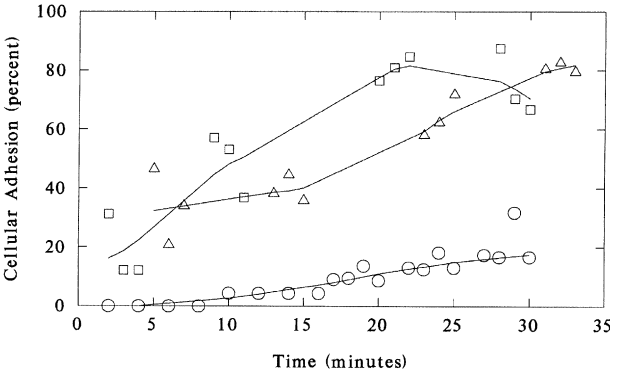

Fig. 3. Quantitative time course of cell adhesion. Cellular adhesion is shown for BS-1 (*circles*), BS-50 (*squares*), and 5 mM RGDS (*triangles*). Data are compiled from multiple experiments.

substrates was observed in BS-50 (Table 1). Furthermore, immunolocalized integrin was punctate, on the outer perimeter of the cells (Fig. 5); it did not appear to be related to the complete adhesion between the bottom of the cell and the substrate observed by interference reflection microscopy.

Cellular Adhesion: Gadolinium-induced Attachment

The addition of a low concentration of $GdCl_3$ to the cell suspension caused rapid and complete cellular attachment on glass: all unattached cells adhered within 1–2 min after the addition of 100–500 μM. $GdCl_3$ (Fig. 6; Table 1). Pretreatment of cells with gadolinium before inoculation (200 μM, 30 min) inhibited adhesion and induced cell aggregation. Gadolinium (100–500 μM) also induced rapid (1–2 min) and complete (100%) cell attachment on both plastic (polystyrene) and pronectin-coated substrates, i.e., on substrates that were non-adhesive for cells in BS-50 in the absence of $GdCl_3$ (Table 1). However, gadolinium was ineffective when the substrate was coated with gelatin. Modification of sugar residues on the surface of the slime cells, by either Con-A or *beta*-galactosidase pre-treatment inhibited gadolinium-induced attachment on glass or plastic (Table 1).

In summary, cellular adhesion is enhanced by higher levels of $MgCl_2$ in the absence of gadolinium, but at a low attachment efficiency. The adhesive mechanism does not appear to involve integrin. When gadolinium is added to the cells, attachment is rapid with high efficiency, and occurs on very different substrates—(glass, plastic (polystyrene) and pronectin-coated substrates—with the exception of gelatin. Adhesion efficiency is inhibited strongly by modification of surface sugar residues by Con-A or *beta*-galactosidase pre-treatment.

Cellular Adhesion: Polystyrene Microsphere Attachment

During the process of cell settling and attachment, polystyrene (plastic) microsphere beads (1 μm dia-

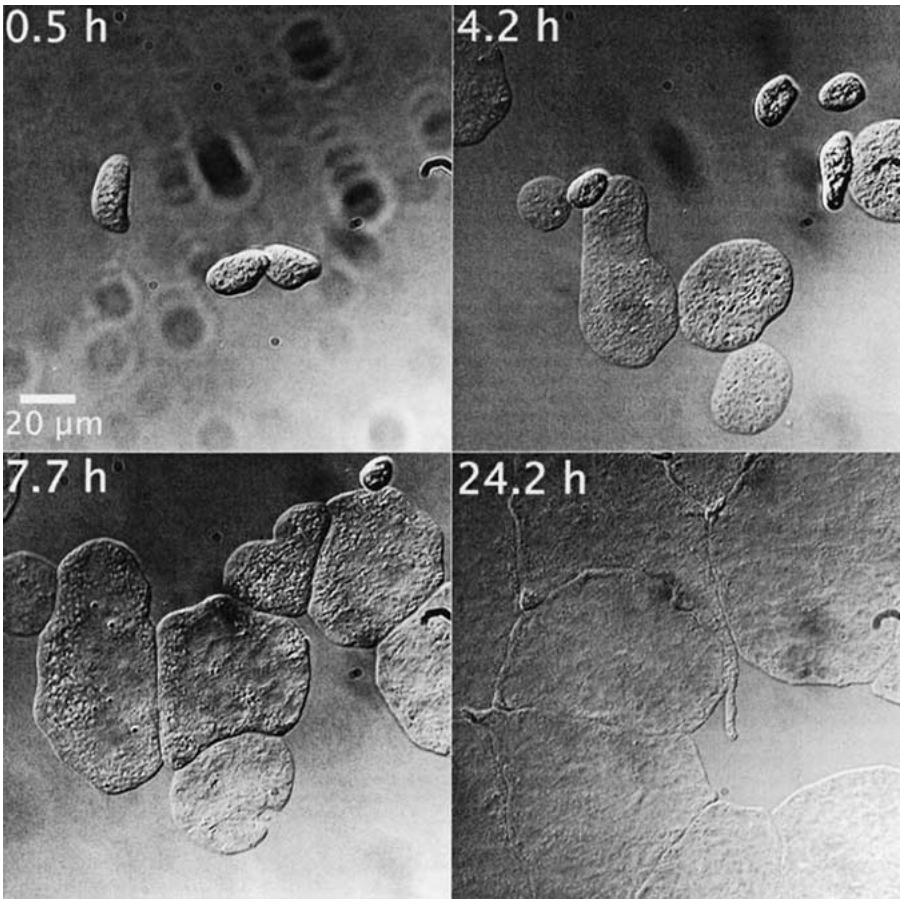

Fig. 4. Long-term phenotype of *slime* cells attached to a glass substrate in BS-50. Differential interference microscopy at the times shown after introduction into the chamber. Note the pseudopodial extension at time 24.2 h. This moved sideways, and retracted over time (*not shown*). These morphologies were described in detail by Trevithick and Galsworthy (1977).

meter) were added to the culture dish. Analogous to cell adhesion to polystyrene culture dishes, the carboxylate-modified polystyrene beads were able to attach to the surface of the slime cells. When they did so, they exhibited motion along the surface, suggesting a dynamic movement of adhesive patches on the surface of the *slime* cells (Fig. 7). An example of adhesive connections to the polystyrene microsphere is shown in Figure 8. Possible endocytotic events were observed (Fig. 8), but very rarely.

Gadolinium-induced Gigaseal Formation in Liposomes

Gigaseals were formed within a few seconds after the pipette touched the GUL surface. No additional suction or application of negative voltage was necessary. The formation of gigaseals was spontaneous and fast, the transition occurred within the recording resolution of 0.5 s.

There was no difference between gigaseal values for GUL and GUL(-S). Application of 100 µM of Gd^{3+} (10 µl from 100 mM stock) caused a 2- to 20-fold increase in seal resistance for both types of liposomes within 0.5–3 min (Table 2). The time course of the gigaseal formation for GUL is shown on Fig. 9.

Discussion

Gigaseal-induced Gigaseal Formation in *Slime* Cells

Sokabe and Sachs (1990) imaged patch-clamped membranes using DIC microscopy and observed a complex architecture that included cytoplasm and vesicles. This complex architecture was confirmed using electron microscopy (Ruknudin et al., 1991). The formation of the gigaseal is believed to require annealing of membrane with the inside glass surface of the patch pipette, after it has been drawn into the pipette by applied suction.

In the case of the *slime* mutant, seal formation in normal bathing solution is very slow (Levina et al., 2002), also observed for gigaseal formation in wild-

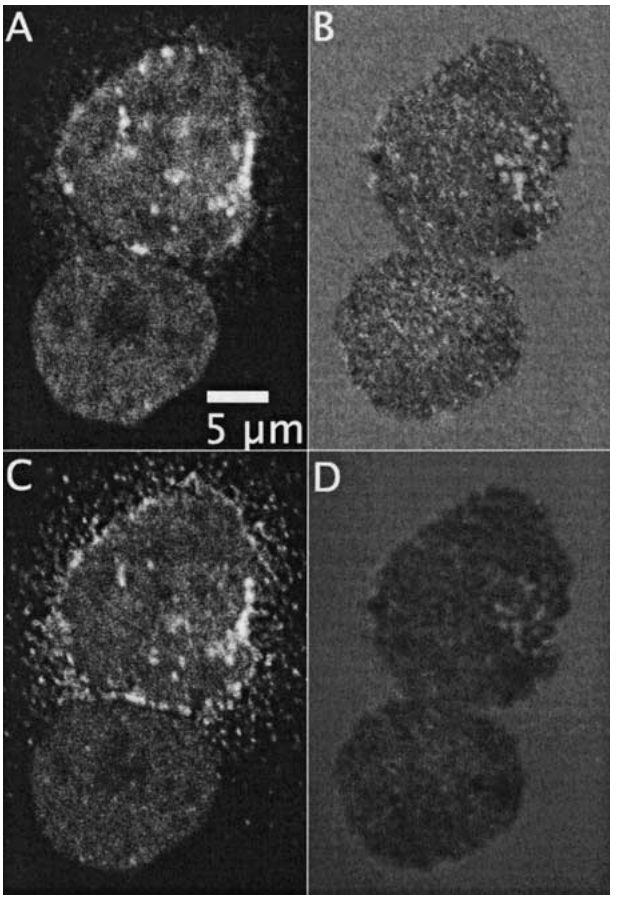

Fig. 5. Integrin localization in adhering *slime* cells. Left panels (*A* and *C*) show fluorescence immunolocalization of integrin. Right panels (*B* and *D*) show interference reflection microscopic images. The upper panels (*A* and *B*) are taken at a plane of focus just above the cell/glass interface, the lower panels (*C* and *D*) are taken at the cell/glass interface.

type protoplasts produced by cell-wall digestion (N.N. Levina and R.R. Lew, unpublished). In previous patch experiments using *slime* (Levina et al., 2002), we observed that high [Mg^{2+}] (50 mM) is important for gigaseal formation. This has been noted by researchers working on bacteria (Martinac et al., 1987). A low frequency of gigaseal formation has also been reported for the slime mold *Dictyostelium discoideum* (Muller & Hartung, 1990), in which gigaseal formation was enhanced by the addition of specific divalent cations. High [Mg^{2+}] (50 mM compared to 1 mM) (Fig. 3, Table 1) also enhances cell adhesion to glass substrates, suggesting that there is a correlation between cell adhesion to substrates and the ability to form gigaseals. In higher plants, a number of studies suggest that low success rates for gigaseal formation can be overcome by minimizing treatment with the enzymes used to digest the cell wall (Vogelzang & Prins, 1992; Elzenga, Keller & Van Volkenburgh, 1993), or even forgoing enzymatic treatment by using laser ablation of the cell wall (Kurkdjian et al., 1993; DeBoer et al., 1994; Henriksen et al., 1996). This suggests that elements enhancing adhesion between the plasma membrane and the patch pipette are either absent or modified during the treatments required to remove the cell wall. In *slime*, the addition of $GdCl_3$ causes rapid gigaseal formation. Based on *slime* cell adhesion to different substrates, gadolinium-induced adhesion is non-specific, since it occurs when the substrate is glass or plastic, hydrophilic and hydrophobic surfaces, respectively.

Effects of Gadolinium on Gigaseal Formation in Liposomes

Our data indicate that the formation of gigaseal contacts between the glass pipette and giant phospholipid liposomes is spontaneous and occurs within a few seconds after the pipette touches a liposome surface. Addition of Gd^{3+} induced a further increase in the seal resistance. The seal formation was not influenced by the presence of the negatively charged PS in the liposomes.

Ermakov et al. (2001) demonstrated that Gd^{3+} interaction with BLM membranes containing PS (but not PC) caused changes in the mechanical properties of the lipid bilayer, so that membrane tension increased. Besides, Gd^{3+} strongly affected dipole potential of the PS membranes, and the effect correlated with the content of the negatively charged PS in the bilayer. In our experiments, we did not find any marked differences in the Gd^{3+} effect on gigaseal formation in liposomes containing or lacking PS. To a certain extent, this may be explained by low pH of the bath solution in our experiments (pH = 5.8 in BS), so that proton ions could probably screen Gd^{3+} binding sites. Apart from this, mechanisms other than a change in the dipole surface component due to the Gd^{3+} absorption have to be involved. Tanaka et al. (2002) demonstrated that Gd^{3+} induced a shape change of giant unilamellar vesicles lacking PS, which was explained by the decrease in the area difference between external and internal monolayers due to the compression of the external monolayer. We also observed the change in *slime* cell shape in the presence of Gd^{3+}.

We suggest that Gd^{3+} exerts multiple effects on the membranes and may interact simultaneously with lipids and polysaccharides. This suggestion is supported by the work of Izu & Sachs (1991) who demonstrated that the successful formation of gigaseals on mouse As4.1 cells became possible after cells had been treated with the inhibitor of extracellular matrix formation, β-D-xyloside.

Adhesion Mechanisms in the *Slime* Mutant of *Neurospora crassa*

Immunocytochemistry suggests that an integrin-like protein is found at growing *N. crassa* hyphal tips

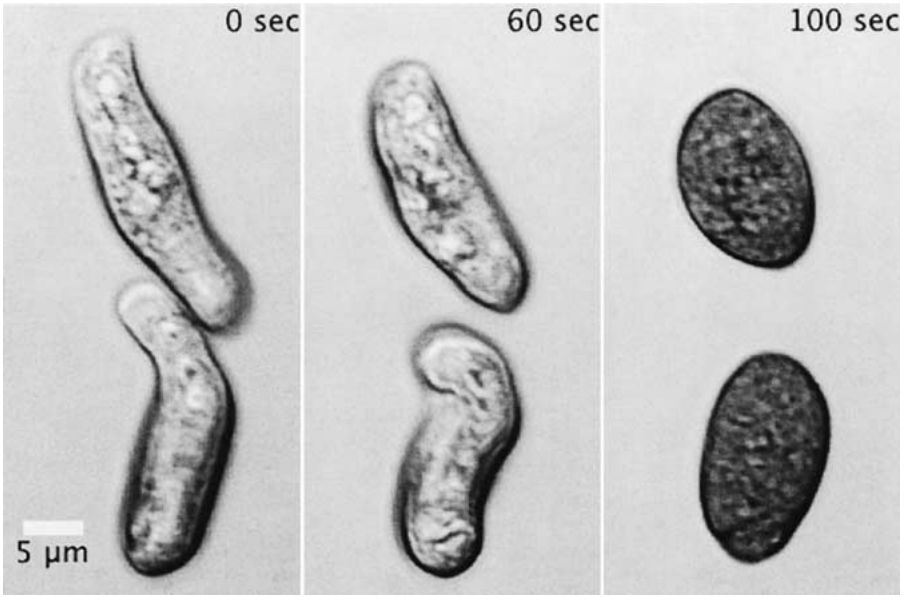

Fig. 6. Gadolinium-induced *slime* cell attachment to glass. Interference reflection microscopy. The slime cells were incubated in BS-50 for 27 minutes, without adhering. Within 100 seconds of adding $GdCl_3$ to a final concentration of 125 μM, the slime cells adhered to the glass substrate.

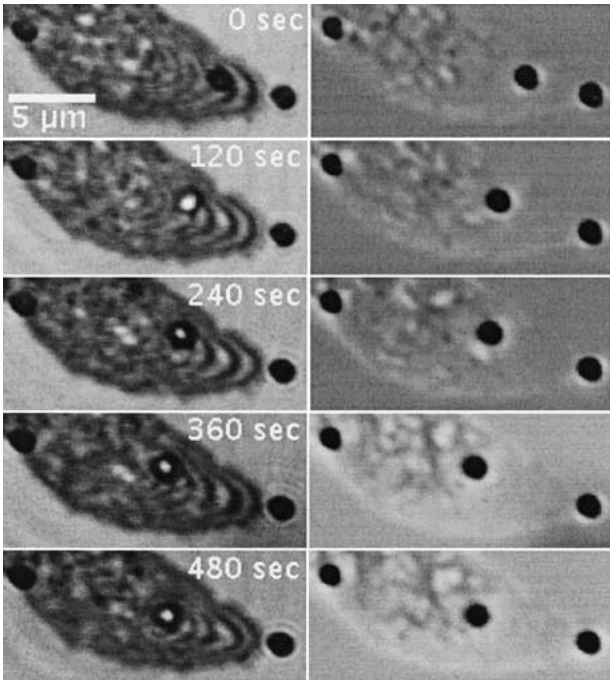

Fig. 7. Polystyrene microsphere adhesion to *slime* cells and microsphere motion on the surface. Images were taken every 120 seconds, at the times shown. The left panels show interference reflection microscopy, the right panels are DIC images. Note that the microsphere is light in the interference reflection microscopic images, indicating that it is on the upper surface of the cell.

(Degousee et al., 2000), and probably plays a role connecting the cell wall to the cytoskeleton (Kaminskyj & Heath, 1995), in addition to other cytoplasm-plasma membrane-cell wall adhesion mechanisms (Bachewich & Heath, 1997). In the fungus *Candida albicans*, an integrin-like protein (Gale et al., 1996) has been implicated in adhesion and pathogenesis (Gale et al., 1998). In the amoeba *Neoparamoeba aestuarina*, RGD, which competes for the integrin binding site, inhibits adhesion to bovine serum albumen-coated substrate (Custodio et al., 1995). Therefore, we used RGDS (and the non-active RGES) pretreatment, and adhesion to gelatin- and pronectin-coated plates, to test whether integrin mediates substrate adhesion. There was no effect of RGDS and RGES pretreatment, and no adhesion to gelatin- and pronectin-coated substrates was observed. There was no co-localization of integrin and the adhesion, based upon immunocytochemical localization of integrin. Although integrin plays a role in fungal walled cells by connecting the hyphal wall to the underlying cytoplasm (Heath, 2001), the gadolinium-induced adhesion to substrate involves a different and distinct mechanism.

The lectin ConA is known to bind to *slime* plasma membrane, stabilizing the membrane into flat sheets during purification for biochemical characterizations (Scarborough, 1975; Trevithick & Galsworthy, 1977; Smith & Scarborough, 1984). In addition, there are reports that gadolinium binds to ConA (Barber, Fuhr & Carver, 1975; Richardson & Behnke, 1978; Barone et al., 1989) and inhibits ConA binding to mannosides (Barone et al., 1989). Therefore, we examined the possibility that sugar residues on the external face of the *slime* plasma membrane mediate adhesion. The inhibitory effect of Con-A and

Table 2. Effect of Gadolinium on gigaseal formation in giant unilamellar liposomes

	GUL control	GUL + Gd	GUL(-S) control	GUL(-S) + Gd
R(Gohm)	9 ± 4 (n=11)	18 ± 12 (n=5)	9 ± 6 (n=10)	21 ± 16 (n=4)
Time the effect appears[1] (s)	36 ± 18	96 ± 48	25 ± 10	113 ± 64

Data are shown as mean ± SD (n). [1]Period between pipette-liposome contact and onset of effect.

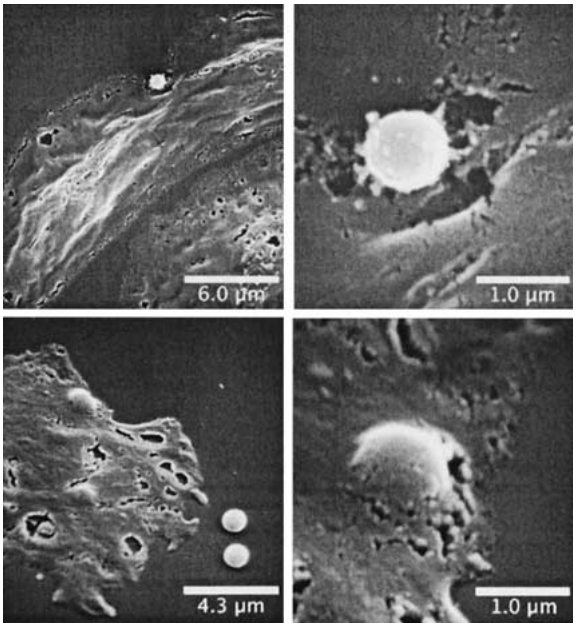

Fig. 8. Scanning electron microscopy showing attached and embedded, possibly endocytosed, polystyrene microspheres. The upper panels show a microsphere adhering to the *slime* cell. Points of contact are clearly visible at higher magnification (*upper right panel*). A putative endocytosed microsphere is shown in the lower panels. It is not certain, even at higher magnification (*lower right panel*), whether the microsphere is *within* the *slime* cell or has been *covered by* the *slime* cell. Endocytosis of *Escherichia coli* spheroplasts by *slime* cells has been reported by Tanaka et al. (1984), but only after treatment with polyvinyl alcohol. We also observed possible endocytosis of the microspheres using either differential interference contrast microscopy or localization of fluorescent microspheres 'inside' Nile Red fluorescently labelled *slime* membranes (*not shown*). Scales are shown for each scanning electron micrograph.

beta-galactosidase on adhesion does indicate that adhesion involves sugar residues. Gigaseal formation does not occur after Con-A treatment (Levina et al., 2002). The actual molecular binding mechanism remains obscure. Others have implicated proteoglycans in gigaseal formation (Olesen, 1995), and direct lipid-glass adhesion also occurs (Tank et al., 1982; Milton & Caldwell, 1990; Opsahl & Webb, 1994). In the case of the *slime* cell, a more likely alternative is sugar-glass adhesion, previously suggested by Sokabe and Sachs (1990).

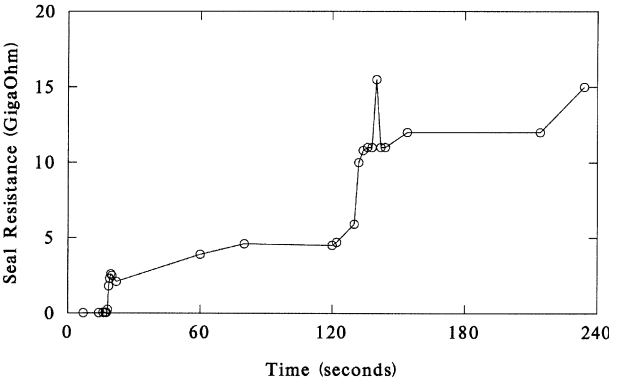

Fig. 9. Gigaseal formation in giant unilamellar liposomes made of PC:PE:PS:Ch (50:10:30:10 w/w). The seal resistance was monitored by measuring the clamping currents evoked by 20-mV voltage steps in voltage-clamp mode. $GdCl_3$ (final concentration 100 μM) was added at 124 s.

The *slime* Mutant of *Neurospora crassa* Is an Amoeboid Cell

The general behavior of the slime cell on substrates exhibits the phenotype of an animal or amoeboid cell (Trevithick & Galsworthy, 1977). Phylogenetically, evidence points to a close relation between the animal and fungal kingdoms (Baldauf & Palmer, 1993). However, as walled cells exhibiting turgor, the wild-type *phenotype* of organisms within the fungal kingdom are far closer to the *phenotype* of organisms within the plant kingdom than they are to organisms in the animal kingdom. Indeed, it is remarkable how many varying types of symbioses and pathogenicity exist between fungal and plant organisms, indicating a closely intertwined evolutionary history (Heckman et al., 2001). The *slime* mutant of *Neurospora crassa* is one of very few examples of a fungal organism exhibiting an amoeboid cell phenotype similar to an animal cell. The other examples are zoospores of Chyridiomycota (a 'true' fungal group) and zoospores of Oomycota (another hyphal organism) (Heath & Steinberg, 1999). The characteristics of *slime* gave us a unique opportunity to examine adhesive mechanisms in the context of gigaseal formation. It is possible that a similar adhesion mechanism occurs during gigaseal formation in animal cells.

This work was supported by a NATO Collaborative Linkage grant (#565370) to A.Y.D-B., R.R.L., and N.N.L., and NSERC Discovery Grants to R.R.L. and LB.H. We thank Tim Bourett for advice on slow freezing techniques for immunocytochemistry. A special thanks to Karen Rethoret, Manager of the Imaging Facility, for her assistance with all aspects of confocal microscopy and scanning electron microscopy.

References

Alex, L.A., Borkovich, K.A., Simon, M.I. 1996. Hyphal development in *Neurospora crassa*: involvement of a two-component histidine kinase. *Proc. Natl. Acad. Sci. USA* **93:**3416–3421

Bachewich, C.L., Heath, I.B. 1997. Differential cytoplasm-plasma membrane-cell wall adhesion patterns and their relationships to hyphal tip growth and organelle motility. *Protoplasma* **200:**71–86

Baldauf, S.L., Palmer, J.D. 1993. Animals and fungi are each other's closest relatives: Congruent evidence from multiple proteins. *Proc. Natl. Acad. Sci. USA* **90:**11558–11562

Barber, B.H., Fuhr, B.J., Carver, J.P. 1975. Magnetic-resonance study of concanavalin-A—identification of a lanthanide binding site. *Biochemistry* **14:**4075–4082

Barone, G., Castronuovo, G., Del, Vecchio, P., Elia, V., Guarrata, P. 1989. Binding of lanthanum and gadolinium ions to concanavalin A studied calorimetrically at 25 degrees C. *J. Mol Recognit.* **2:**147–151

Bourett, T.M., Czymmek, K.J., Howard, R.J. 1998. An improved method for affinity probe localization in whole cells of filamentous fungi. *Fung. Genet. Biol.* **24:**3–13

Bowman, B.J., Slayman, C.W. 1977. Characterization of plasma membrane adenosine triphosphatase of *Neurospora crassa*. *J. Biol. Chem.* **252:**3357–3363

Custodio, M.R., Imsiecke, G., Borojevic, R., Rinkevich, B., Rogerson, A., Muller, W.E. 1995. Evolution of cell adhesion systems: evidence for Arg-Gly-Asp-mediated adhesion in the protozoan *Neoparamoeba aestuarina*. *J. Euk. Microbiol.* **42:**721–724

DeBoer, A.H., Van Duijn, B., Giesberg, P., Wegner, L., Obermeyer, G., Kohler, K., Linz, K.W. 1994. Laser microsurgery - A versatile tool in plant (electro)physiology. *Protoplasma* **178:**1–10

Degousee, N., Gupta, G.D., Lew, R.R., Heath, I.B. 2000. A putative spectrin-containing membrane skeleton in hyphal tips of *Neurospora crassa*. *Fung. Genet. Biol.* **30:**33–44

Elzenga, J.T.M., Keller, C.P., Van Volkenburgh, E. 1993. Patch clamping protoplasts from vascular plants. Method for the quick isolation of protoplasts having a high success rate of gigaseal formation. *Plant Physiol.* **97:**1573–1575

Emerson, S. 1963. Slime, a plasmodioid variant of *Neurospora crassa*. *Genetica* **34:**162–182

Ermakov, Y.A., Averbalch, A.Z., Yusipovich, A.I., Sukharev, S. 2001. Dipole potentials indicate restructuring of the membrane interface induced by gadolinium and beryllium ions. *Biophys. J.* **80:**1851–1862

Gale, C., Finkel, D., Tao, N., Meinke, M., McClellan, M., Olson, J., Kendrick, K., Hostetter, M. 1996. Cloning and expression of a gene encoding an integrin-like protein in *Candida albicans*. *Proc. Natl. Acad. Sci. USA* **93:**357–361

Gale, C.A., Bendel, C.M., McClellan, M., Hauser, M., Becker, J.M., Berman, J., Hostetter, M.K. 1998. Linkage of adhesion, filamentous growth, and virulence in *Candida albicans* to a single gene, INT1. *Science* **279:**1355–1358

Heath, I.B. 2001. Bridging the divide: Cytoskeleton-plasma membrane-cell wall interactions in growth and development. *In:* Howard, R.J., Gow, N.A.R. (editors) The Mycota VIII Biology of the Fungal Cell.Springer-Verlag, Berlin and Heidelberg, pp 210–223

Heath, I.B., Steinberg, G. 1999. Mechanisms of hyphal tip growth: tube dwelling amebae revisited. *Fung. Genet. Biol.* **28:**79–93

Heckman, D.S., Geiser, D.M., Eidell, B.R., Stauffer, R.L., Kardos, N.L., Hedges, S.B. 2001. Molecular evidence for the early colonization of land by fungi and plants. *Science* **293:**1129–1133

Henriksen, G.H., Taylor, A.R., Brownlee, C., Assmann, S.M. 1996. Laser microsurgery of higher plant cell walls permits patch-clamp access. *Plant Physiol.* **110:**1063–1068

Hynes, R.O. 1992. Integrins: Versatility, modulation, and signaling mechanisms. *Cell* **69:**11–25

Izu, Y.C., Sachs, F. 1991. Inhibiting synthesis of extracellular matrix improved patch clamp seal formation. *Pfluegers Arch.* **419:**218–220

Izzard, C.S., Lochner, L.R. 1976. Cell-to-substrate contacts in living fibroblasts: an interference reflexion study with an evaluation of the technique. *J. Cell Sci.* **21:**129–159

Kaminskyj, S.G.W., Heath, I.B. 1995. Integrin and spectrin homologs and cytoplasm-wall adhesion in tip growth. *J. Cell Sci.* **108:**849–856

Kurkdjian, A., Leitz, G., Maniault, P., Harim, A., Greulich, K.O. 1993. Nonenzymatic access to the plasma-membrane of *Medicago* root hairs by laser microsurgery. *J. Cell Sci.* **105:**263–268

Levina, N.N., Dunina-Barkovskaya, A.Y., Shabala, S., Lew, R.R. 2002. Blue light modulation of ion transport in the slime mutant of *Neurospora crassa*. *J. Membrane Biol.* **188:**213–226

Martinac, B., Buechner, M., Delcour, A.H., Adler, J., Kung, C. 1987. Pressure-sensitive ion channel in *Escherichia coli*. *Proc. Natl. Acad. Sci. USA* **84:**2297–2301

Milton, R.L., Caldwell, J.H. 1990. How do patch clamp seals form? A lipid bleb model. *Pfluegers Arch.* **416:**758–762

Muller, U., Hartung, K. 1990. Properties of three different ion channels in the plasma membrane of the slime mold *Dictyostelium discoideum*. *Biochim. Biophys. Acta* **1026:**204–212

Olesen, S.P. 1995. Cell membrane patches are supported by proteoglycans. *J. Membrane Biol.* **144:**245–248

Opas, M. 1978. Interference reflection microscopy of *Amoeba proteus*. *J. Microsc.* **112:**215–221

Opsahl, L.R., Webb, W.W. 1994. Lipid-glass adhesion in gigasealed patch-clamped membranes. *Biophys. J.* **66:**75–79

Perkins, D.D., Radford, A., Newmeyer, D., Bjorkman, M. 1982. Chromosomal loci of *Neurospora crassa*. *Microbiol. Rev.* **46:**426–570

Reinhardt, M.O. 1892. Das Wachsthum der Pilzhyphen. *Jahrb. Wiss. Bot.* **23:**479–566

Richardson, C.E., Behnke, W.D. 1978. Physical studies of lanthanide binding to concanavalin A. *Biochim. Biophys. Acta* **534:**267–274

Ruknudin, A., Song, M.J., Sachs, F. 1991. The ultrastructure of patch-clamped membranes: A study using high voltage electron microscopy. *J. Cell Biol.* **112:**125–134

Sachs, F., Qin, F. 1993. Gated, ion-selective channels observed with patch pipettes in the absence of membranes: novel properties of a gigaseal. *Biophys. J.* **65:**1101–1107

Scarborough, G.A. 1975. Isolation and characterization of *Neurospora crassa* plasma membranes. *J. Biol. Chem.* **250:**1106–1111

Schumacher, M.M., Enderlin, C.S., Selitrennikoff, C.P. 1997. The osmotic-1 locus of *Neurospora crassa* encodes a putative histidine kinase similar to osmosensors of bacteria and yeast. *Curr. Microbiol.* **34:**340–347

Smith, R., Scarborough, G.A. 1984. Large-scale isolation of the *Neurospora* plasma membrane H^+ -ATPase. *Anal. Biochem.* **138:**156–163

Sokabe, M., Sachs, F. 1990. The structure and dynamics of patch-clamped membranes: A study using differential interference contrast light microscopy. *J. Cell Biol.* **111:**599–606

Tanaka, N., Fukunaga, Y., Hasezawa, S., Syono, K., Matsui, C. 1984. Endocytotic uptake of *Escherichia coli* spheroplasts by *Neurospora crassa slime cells*. *Appl. Microbiol. Biotech.* **19:**296–299

Tanaka, T., Tamba, Y., Masum, S.M., Yamashita, Y., Yamazaki, M. 2002. La^{3+} and Gd^{3+} induce shape change of giant unilamellar vesicles of phophatidylcholine. *Biochim. Biophys. Acta* **1564:**173–182

Tank, D.W., Miller, C., Webb, W.W. 1982. Isolated-patch recording from liposomes containing functionally reconstituted chloride channels from *Torpedo* electroplax. *Proc. Natl. Acad. Sci. USA* **79:**7749–7753

Trevithick, J.A., Galsworthy, P.R. 1977. Morphology of *Slime* variants of *Neurospora crassa* growing on a glass surface in liquid medium. 1. Under normal conditions and 2. In the presence of inhibitors. *Arch. Microbiol.* **115:**109–118

Vogel, H. 1956. A convenient growth medium for *Neurospora*. *Microb. Genet. Bull.* **13:**42–46

Vogelzang, S.A., Prins, H.B.A. 1992. Plasmalemma patch clamp experiments in plant root cells: procedure for fast isolation of protoplasts with minimal exposure to cell wall degrading enzymes. *Protoplasma* **171:**104–109